

Electronic specific heat in the pairing pseudogap regime

C. P. Moca and Boldizsár Jankó

Materials Science Division, Argonne National Laboratory, Argonne, Illinois 60439
and Department of Physics, University of Notre Dame, Notre Dame, Indiana 46556

(Received 9 May 2001; published 3 January 2002)

When pairing correlations in a quasi-two-dimensional electron system induce a pseudogap in the single-particle density of states, the specific heat must also contain a sizable pair contribution. The theoretically calculated specific heat for such a system is compared to the experimental results of Loram and his collaborators for underdoped $\text{YBa}_2\text{Cu}_3\text{O}_{6+x}$ and $\text{La}_{2-x}\text{Sr}_x\text{CuO}_4$ samples. The size and doping dependence of the extracted pseudogap energy scale for both materials is comparable to the values obtained from a variety of other experiments.

DOI: 10.1103/PhysRevB.65.052503

PACS number(s): 74.25.Bt, 74.25.Dw

I. Introduction. The gradual, but substantial loss of low-energy single-particle states in the normal state of underdoped cuprate samples has been by now documented by a large number of experiments.¹ The onset of the pseudogap regime is captured most clearly by spectroscopic probes that couple predominantly to the single-particle excitations, such as tunneling² and angle-resolved photoemission spectroscopy (ARPES).³ All theoretical expectations, however, point towards some sort of many-particle phenomenon behind the pseudogap effect and imply observable changes in collective electronic properties.⁴ Traditional probes of collective degrees of freedom, such as inelastic neutron scattering,⁵ Raman scattering,⁶ and optical conductivity,¹ were used extensively on pseudogapped samples, while new experiments, such as higher order tunneling spectroscopy,⁷ were also proposed. Despite such remarkable accumulations of high-quality experimental data a consensus has yet to emerge regarding the origin of the collective effect causing the pseudogap.

One of the earliest experimental indications of normal-state anomalies in underdoped cuprates came not from spectroscopic but from thermodynamic measurements. Loram and his collaborators found⁸ that the coefficient of the electronic heat capacity $\gamma_{\text{el}}(T) = C_{\text{el}}(T)/T$ of underdoped samples is no longer constant in temperature, as it is for the optimal and overdoped crystals and as one would expect from a normal Fermi liquid. Instead, $\gamma_{\text{el}}(T)$ shows a broad maximum at a crossover temperature T^* which is doping dependent and typically much higher than the superconducting transition temperature T_c . As T is lowered below T^* , $\gamma_{\text{el}}(T)$ decreases significantly before the temperature reaches T_c . Despite the fact that these specific heat measurements have been available for some time, there is no systematic study of these data within any theoretical framework of a proposed pseudogap scenario. The purpose of this paper is to provide such an analysis within a pairing fluctuation framework.

There are several reasons why the results of these thermodynamic measurements deserve a detailed theoretical analysis. First, there is ample experimental data on the most extensively studied classes of cuprate superconductors, $\text{YBa}_2\text{Cu}_3\text{O}_{6+x}$, $\text{La}_{2-x}\text{Sr}_x\text{CuO}_4$,⁸ and recently $\text{Bi}_2\text{Sr}_2\text{CaCu}_2\text{O}_{8+x}$,⁹ for a remarkably wide range of doping.

This makes it possible to single out and to concentrate the theoretical study on the universal features mentioned above. Second, these thermodynamic measurements couple to all thermally excitable modes, irrespective of their single-particle or collective character. In tunneling and photoemission higher-order excitations, such as pair excitations, may be detected only through their convoluted influence on the single-particle spectrum. Thus, in contrast to any theoretical analysis of single-particle spectroscopy data, where one seems to have a choice⁴ in selecting the collective phenomena causing the pseudogap, comparison between theory and thermodynamic data provides a consistency check, once the choice has been made.

In this article we perform such a consistency check for a simple pair fluctuation model of the pseudogap regime, introduced by Vilk and Tremblay.¹⁰ We opted for this formulation because it permits an essentially analytical treatment, and therefore the analysis is not obscured by the numerical difficulties ubiquitous in most other incarnations of the pair fluctuation scenario.¹¹ We believe, however, that the results we obtained have a range of relevance that goes beyond the present formulation and it is characteristic of a larger class of pair fluctuation models for the pseudogap.¹²

In our calculation we consider, beside the usual single-particle contribution,¹³ the contribution of the fluctuating pairs. We show that (a) it has the same order of magnitude as the single particle contribution and (b) it is essential for explaining the *universal* presence of a broad hump in the specific heat data. In what follows we first present the main theoretical framework and then report a detailed analysis of the experimental data within this framework. The central result of our analysis is the doping dependence of the *pairing* pseudogap energy extracted from specific heat data, which compares well with the doping dependence of the pseudogap scale inferred from a variety of other measurements.

II. Pairing contribution. For calculation of the pairing contribution we start with the usual expression of the grand potential for pair fluctuations:¹⁴

$$\Omega_p(T) = -T \sum_{\mathbf{k}, \omega_n, \sigma} \ln[1 - g\chi(\mathbf{q}, \omega_n)], \quad (1)$$

where $\chi(\mathbf{q}, \omega_n)$ is the pairing susceptibility. In what follows we will consider only the noninteracting, bare susceptibility

$$\chi(\mathbf{q}, \omega_n) = \frac{1}{\beta} \sum_{\mathbf{k}, \zeta_m} G^0(\mathbf{k} + \mathbf{q}, i\zeta_m + i\omega_n) G^0(\mathbf{k}, i\zeta_m), \quad (2)$$

where $[G^0(\mathbf{k}, i\zeta_n)]^{-1} = i\zeta_n - \epsilon_{\mathbf{k}}$. Here $\epsilon_{\mathbf{k}}$ is the single-particle dispersion and $\zeta_n = (2n+1)\pi/\beta$ is the fermionic Matsubara frequency. The summation in Eq. (1) is done over the pair momentum \mathbf{q} , bosonic Matsubara frequencies $\omega_n = 2\pi n/\beta$, and spin σ . We consider the renormalized classical regime corresponding to $\omega_n \sim 0$. Classical fluctuations give in two dimensions the dominant contribution to the self-energy at low frequencies. Quantum fluctuations ($\omega_n \neq 0$) are important only at low temperatures and are irrelevant for temperatures $T_c < T < T^*$. Thus, in the renormalized classical regime the susceptibility is given by the relation

$$1 - g\chi(\mathbf{q}) = \xi(T)^{-2} + q^2. \quad (3)$$

Here $\xi(T)$ is the correlation length, which in the classical regime is constrained to grow faster than the thermal de Broglie wavelength $\xi(T) > \xi_B = \hbar v_F / k_B T$. However, a temperature independent pseudogap as seen in ARPES (Ref. 3) can be obtained in this model if the calculated gap $\Delta^2 = g/2\pi T \ln(\xi/\xi_0)$ is constant in T . The ARPES data, therefore, constrain $\xi(T)$ to be of the form $\xi(T) = \xi_0 \exp(-T/T^*)$. We will show that this form of $\xi(T)$ results in a broad maximum in $\gamma(T)$ around T^* in agreement with the data. The characteristic temperature scale T^* is set by the coupling strength g and pseudogap Δ (note that in this notation g has units of energy):

$$k_B T^* = \frac{2\pi}{g} \Delta^2. \quad (4)$$

T^* can also be identified with the onset of pseudogap behavior. In principle both Δ and g can be doping dependent. The dimensionless specific heat coefficient $\gamma(T) \equiv c_v(T)/k_B^2 T N(0)$ can be obtained directly from Eq. (1) according to the thermodynamic relation $c_v(T) = -T \partial^2 \Omega / \partial T^2$. The result for the *pair contribution* is

$$\gamma_p(T) = 16\pi A \left(\frac{T^*}{T} \right)^3 e^{-(2T^*/T)} \left(1 + \frac{T}{2T^*} \ln \Lambda \right). \quad (5)$$

In strictly two dimensions the integration of the pair momenta needs to be regularized by introducing an upper cutoff Λ . In practice, however, the materials we are interested in have a large, but finite, c -axis anisotropy, which naturally cuts off the pair momenta $\Lambda \sim \xi_0/d_c$ where d_c is the interlayer distance. In Eq. (5), $A \sim [\xi_0^2 k_B T^* N(0)]^{-1}$ is the parameter that governs the relative importance of the pairing contribution. The characteristic feature of the pairing contribution to the specific heat is a broad hump near a temperature $T \sim T^*$. This contribution in general and the hump feature in particular are important for obtaining a good fit to the experimental data.

III. Single particle contribution. The single-particle contribution to the grand potential is given by¹³

$$\Omega_s(T) = -T \sum_{\mathbf{k}, \omega_n, \sigma} \{ \ln[G^{-1}(\mathbf{k}, \omega_n)] - \Sigma(\mathbf{k}, \omega_n) \cdot G(\mathbf{k}, \omega_n) \}. \quad (6)$$

For the present purposes we identify the self-energy $\Sigma(\mathbf{k}, \omega_n)$ in the above expression with the pairing self-energy¹⁰ of the renormalized classical regime:

$$\Sigma(\mathbf{k}, \omega_n) = \frac{\Delta^2}{i\omega_n + \epsilon_{\mathbf{k}}}, \quad (7)$$

where Δ is the pseudogap energy scale. For the dimensionless specific heat coefficient coming from this contribution we obtained the result

$$\gamma_s(T) = \frac{2\pi^2}{3} + \int_0^\infty \left(\frac{N(x, d)}{N(0)} - 1 \right) f(x) [1 - f(x)] x^3. \quad (8)$$

In Eq. (8) we introduced the following notation: $x = E_{\mathbf{k}}/k_B T$, $d = \Delta/k_B T$, $E_{\mathbf{k}} = \sqrt{\epsilon_{\mathbf{k}}^2 + \Delta^2}$, and $f(x) = (e^x + 1)^{-1}$. As indicated by angle-resolved photoemission spectra³ taken in the pseudogap regime, the single-particle states in this regime are very broad. During analysis of the specific heat data we found that even for near-optimal doping an intrinsic broadening of the single-particle states must be considered in order to obtain a reasonable account of the data based on the single particle contribution (8). The importance of broadening in the single-particle states becomes even more apparent when our analysis is performed on data taken on underdoped samples. This trend is again consistent with that observed in ARPES.¹⁵ We therefore introduce a phenomenological broadening of the single-particle density of states in the simple form

$$\frac{N(x, d)}{N(0)} = \left| \text{Re} \frac{x - i\gamma}{\sqrt{(x - i\gamma)^2 + d^2}} \right| \quad (9)$$

and $\gamma = \Gamma/k_B T$ [not to be confused with $\gamma_p(T)$ or $\gamma_s(T)$]. We would like to note that while the broadening Γ is essential for treating the single-particle contribution it is less important for the qualitative behavior of the pair contribution $\gamma_p(T)$ as function of temperature. The total contribution to the specific heat coefficient is

$$\gamma_{el}(T) = \gamma_s(T) + \gamma_p(T). \quad (10)$$

IV. Relative magnitude of the pairing and single particle contributions. From the results obtained in Eqs. (4) and (7) we see that the relative importance of pairing contribution $\gamma_p(T)$ compared to the usual contribution $\gamma_s(T)$ is governed by the parameter $A \sim [\xi_0^2 k_B T^* N(0)]^{-1}$. Using $\xi_0 \sim 10a$, $T^* \sim 100$ K, and typical density of states (for example, from ARPES data we get 3 states/eV per Cu-O in a unit cell,³) we find that γ_p and γ_s are comparable in magnitude: $\gamma_p(T) \sim \gamma_s(T)$. In contrast, for a superconductor with long coherence length such as Al ($\xi_{Al} \sim 100\xi_{YBCO}$) the pairing contribution $\gamma_p(T)$ is entirely negligible.

V. Comparison with the experiment. A typical comparison of the experimental data with the theoretical result is pre-

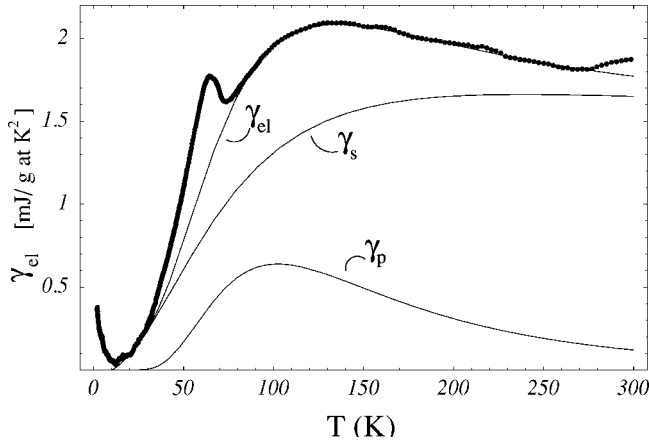


FIG. 1. Fit to the experimentally measured specific heat of $\text{YB}_2\text{Cu}_3\text{O}_{6.73}$ (dots) using the theoretically calculated single-particle and pairing contributions (lines). Note that the single-particle contribution $\gamma_s(T)$ cannot reproduce the hump and the pairing term $\gamma_p(T)$ is necessary.

sented in Fig. 1. Throughout our fitting procedure, the fitting parameters were Δ and Γ only. All other parameters are estimated and fixed as explained in details below. The single-particle and pairing contributions are shown separately in order to emphasize the relative size and the importance of *both* terms. The single particle contribution monotonically increases with increasing temperature and by itself cannot explain the hump observed in the experimental data. If, however, the pairing contribution $\gamma_p(T)$ (with maximum near T^*) is included, the fit is reasonable.¹⁶ During the fitting procedure only the normal state ($T > T_c$) specific heat values are used. Instead of using the ARPES density of states $N(0)$ for every doping, an overall factor of order of 0.1 and dimensions of mJ/gat K^2 is used to scale the dimensionless theoretical expressions to the data at optimal doping. Once this constant is obtained as described above (0.14 mJ/gat K^2 for $\text{La}_{2-x}\text{Sr}_x\text{CuO}_4$ and 0.23 mJ/gat K^2 for $\text{YBa}_2\text{Cu}_3\text{O}_{6+x}$) it is no longer a fitting parameter and remains fixed for all doping levels. An interesting result emerges from the present analysis. The best fit is obtained if $T^*(x)$ is taken to be *proportional* to $\Delta(x)$: $T^* \sim \Delta(x)$; thus we constrained T^* to obey this relation. This proportionality has also been indicated by several other groups,¹⁸ based on a scaling analysis of various experimental data, and an approximate ratio of $\Delta = 1.5T^*$ has been found, similar to our finding. Equation (3) implies, at least for the present pair fluctuation formalism, that the ratio $\Delta(x)/g(x)$ is independent of doping. The parameter A depends on T^* in a simple way, so A is a function of Δ and not a fitting parameter. The doping dependence of the density of states enters through Eq. (9). When considering both single-particle and pair contributions, a direct comparison of the theoretical results and the experimental data can be performed. The results are presented in Fig. 2 for $\text{YBa}_2\text{Cu}_3\text{O}_{6+x}$, and in Fig. 3 for $\text{La}_{2-x}\text{Sr}_x\text{CuO}_4$.¹⁷ The phase diagram obtained from the extracted values of the pairing pseudogap Δ and the experimental transition tempera-

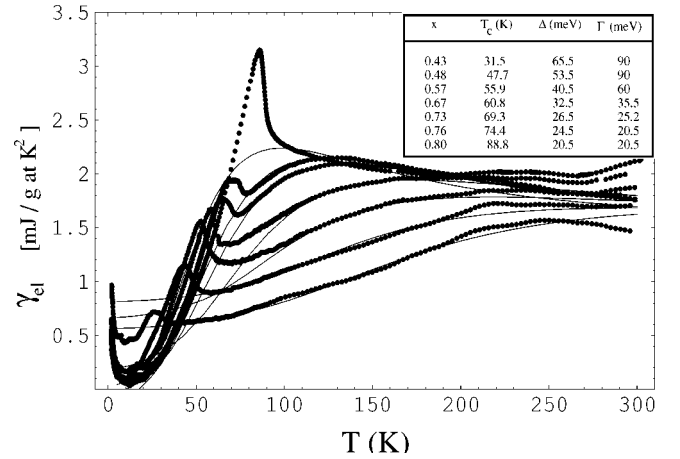


FIG. 2. Specific heat data (dots) for $\text{YB}_2\text{Cu}_3\text{O}_{6+x}$ for a wide range of doping (from below) $x=0.43, 0.48, 0.57, 0.67, 0.73, 0.76$ and 0.80 and the corresponding theoretical curves (lines). The inset gives extracted values for Δ and Γ .

tures is presented in Fig. 4. Here we use reduced quantities (normalized to their value at optimal doping) to present on the same scale the experimentally measured critical temperatures T_c of $\text{YBa}_2\text{Cu}_3\text{O}_{6+x}$ and $\text{La}_{2-x}\text{Sr}_x\text{CuO}_4$ compounds and the corresponding pairing pseudogap scale Δ extracted from data. Thus the doping dependence of the $\Delta(x)/\Delta(x_{max})$ coincides with doping dependence of $T^*(x)/T^*(x_{max})$. The broadening $\Gamma(x)$ increases with decreasing the doping, which is again in qualitative agreement with the ARPES results.^{3,14}

VI. Conclusion. We presented a systematic theoretical analysis of the electronic specific heat in the pseudogap state. While this analysis was performed within the classical pair fluctuation framework for the pseudogap, we suspect that the general features of the results are relevant for a large class of pairing fluctuation scenarios.

The main results of this analysis can be summarized as follows: (i) both the single-particle and pair contributions are of the same order of magnitude and needed to fit the specific

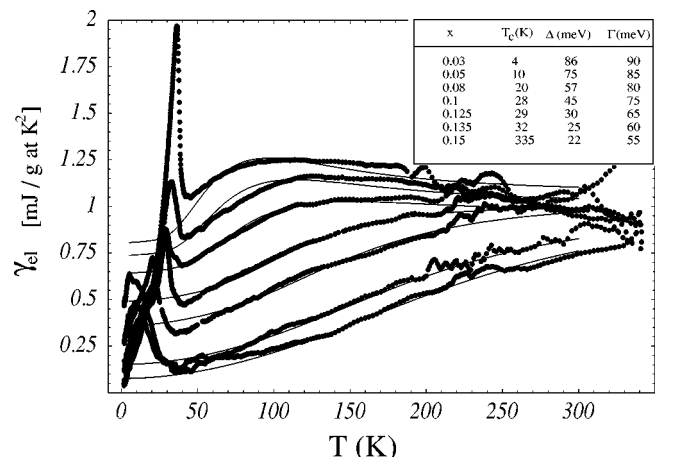


FIG. 3. Same as in Fig. 2, but now for $\text{La}_{2-x}\text{Sr}_x\text{CuO}_4$ [$x=0.03, 0.05, 0.084, 0.1, 0.125, 0.135, \text{ and } 0.15$].

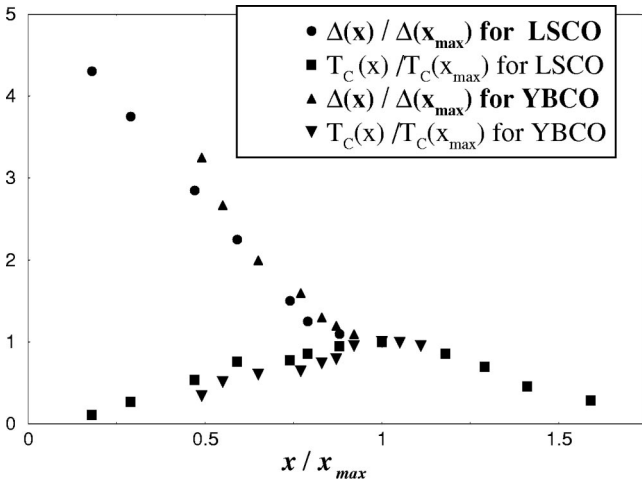


FIG. 4. Doping dependence of the pairing pseudogap Δ extracted from specific heat and of the critical temperature T_c for $\text{YBa}_2\text{Cu}_3\text{O}_{6+x}$ and $\text{La}_{2-x}\text{Sr}_x\text{CuO}_4$.

heat data of pseudogapped samples, and (ii) the electronic specific heat data of underdoped cuprate samples have several universal features that are well captured by our pair fluctuation model. Our analysis of the experimental data yielded a pairing pseudogap energy scale $\Delta(x)$ that has a magnitude and doping dependence which is similar to the pseudogap energy scales extracted from other experiments (cf. Fig. 5). Our main result is the phase diagram presented in Fig. 4.

This work benefited very much from Dr. John W. Loram's

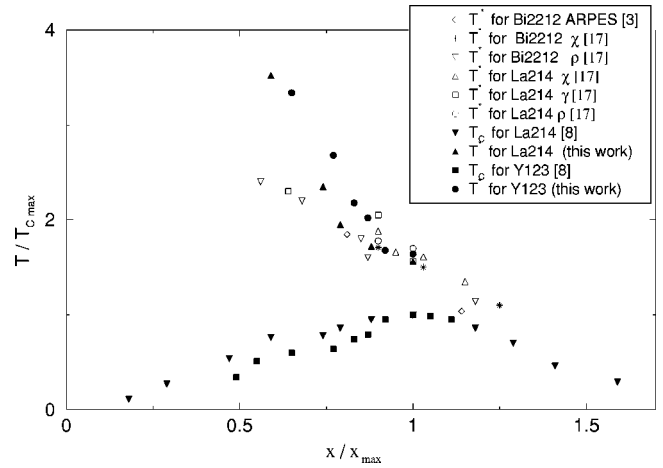


FIG. 5. T^* and T_c doping dependence measured as ARPES, γ , and χ for $\text{YBa}_2\text{Cu}_3\text{O}_{6+x}$, $\text{La}_{2-x}\text{Sr}_x\text{CuO}_4$, and $\text{Bi}_2\text{Sr}_2\text{CaCu}_2\text{O}_{8+x}$.

kind offer to make his specific heat data⁸ available and from several discussions on this issue with him and Dr. Jeffrey Tallon. We would also like to thank Professor Alexei A. Abrikosov, Dr. Ioan Kosztin, Professor Migaku Oda, Professor John Zasadzinski, and especially Dr. Michael R. Norman for helpful discussions. This research was supported in part by the NSF under Grant No. DMR91-2000 (administrated through the Science and Technology Center for Superconductivity) and the U.S. DOE, BES, under Contract No. W-31-109-ENG-38.

¹See, for example, T. Timusk and B. Stratt, Rep. Prog. Phys. **62**, 61 (1999), and references therein.
²Ch. Renner *et al.*, Phys. Rev. Lett. **80**, 3606 (1980); Ch. Renner *et al.*, *ibid.* **80**, 149 (1998); L.H. Greene *et al.*, J. Phys. Chem. Solids **59**, 2021 (1998); N. Miyakawa *et al.*, Phys. Rev. Lett. **83**, 1018 (1999); J.Y.T. Wei *et al.*, *ibid.* **81**, 2542 (1998).
³M.R. Norman *et al.*, Nature (London) **392**, 157 (1998); H. Ding *et al.*, *ibid.* **382**, 51 (1996); A.G. Loeser *et al.*, Science **273**, 325 (1996).
⁴Proceedings of the 6th M²SHTCS Houston, Texas, 2000, Physica C **341-348** (2000).
⁵H.F. Fong *et al.*, Phys. Rev. B **61**, 14 773 (2000); H.F. Fong *et al.*, Phys. Rev. Lett. **78**, 713 (1997).
⁶G. Blumberg *et al.*, Science **278**, 1427 (1997); G. Blumberg and M.V. Klein, Physica B **280**, 180 (2000).
⁷B. Jankó *et al.*, Phys. Rev. Lett. **82**, 4304 (1999).
⁸J.W. Loram *et al.*, J. Supercond. **7**, 234 (1994); J.W. Loram *et al.* (unpublished).
⁹J.W. Loram *et al.*, Physica C **341**, 831 (2000).
¹⁰Y.M. Vilks and A.M.S. Tremblay, J. Phys. I **7**, 1309 (1997).
¹¹See M. Randeria, in *Models and Phenomenology for Conventional and High Temperature Superconductivity*, edited by G.

Iadonisi *et al.*, (IOS Press, Amsterdam, 1999), p. 54.
¹²C.O. Chen *et al.*, Phys. Rev. B **63**, 184519 (2001); see also E. Babaev, *ibid.* **63**, 172502 (2001).
¹³A.A. Abrikosov *et al.*, *Methods of Quantum Field Theory in Statistical Physics*, (Dover, New York, 1963).
¹⁴P. Nozières and S. Schmitt-Rink, J. Low Temp. Phys. **59**, 195 (1985).
¹⁵Note that in contrast to ARPES, scanning tunneling microscopy (STM) measurements do not see the increase in linewidth with underdoping. We believe this discrepancy is due to the local STM versus global nature of the two probes.
¹⁶Note that in our framework $T_c=0$. We do not address the position and magnitude of the specific heat anomaly near the experimentally observed T_c .
¹⁷Since the very recent specific heat data, Fig. 4 taken on $\text{Bi}_2\text{Sr}_2\text{CaCu}_2\text{O}_{8+x}$ are similar with the one in Figs. 2 and 3, we anticipate that the analysis of $\text{Bi}_2\text{Sr}_2\text{CaCu}_2\text{O}_{8+x}$ data will yield qualitatively identical results to the ones obtained here for $\text{YBa}_2\text{Cu}_3\text{O}_{6+\delta}$ and $\text{La}_{2-x}\text{Sr}_x\text{CuO}_4$.
¹⁸T. Matsuzaki *et al.*, J. Phys. Chem. Solids **62**, 29 (2001); M. Kugler *et al.*, Phys. Rev. Lett. **86**, 4911 (2001).